

Copper Losses Studying Using a New Real Time V/f Scalar Control Approach

Mohammed S. Hasan

Department of Power and Electrical
Machine
College of Engineering, University
of Diyala
Diyala, Iraq
mssh6144@gmail.com,

Mohammed D. Albakhait

Department of Electrical Power
Engineering Techniques
Electrical Engineering Technical
College, Middle Technical
University
Baghdad, Iraq
mohammedalbakhait@mtu.edu.iq

Al Mahturi F. Sharaf

Department of Robotics and
Automation of Industrial Systems
Saint Petersburg Electrotechnical
University "LETI"
Saint-Petersburg, Russia
heroiraq@mail.ru

Ahmed I. Jaber

Department of Robotics and
Automation of Industrial Systems,
Saint Petersburg Electrotechnical
University "LETI"
Saint-Petersburg, Russia
m-ph-2011@hotmail.com

Abstract—The paper presents an investigation of copper losses studying of Brushless Doubly-Fed Reluctance Machine supported with Real time results based dSPACE 1103 hardware application and its features to prove the theoretical approach of driver capabilities of Brushless Doubly Fed Reluctance machine at multi-speed in induction and synchronous modes. Moreover, to overcome of these challenges, it needs modernizing the control algorithms strategy. Also, to follow an exciting mode improved the flexibility in speed performance requires more of observation. Scalar control is considered the one of qualified control theories with certain Boost voltage Theory that brings a significant improvement to the performances control algorithm supported BDFRM features. Whereas, this strategy can be used to confirm BDFRM's ability with FOC to manipulate multiple control algorithms that offer this machine an optimal solution instead of induction machine, synchronous machine and permanent magnet synchronous machine.

Keywords—Brushless Doubly-fed Reluctance Machine, V/f Constant, Scalar Control Algorithm, Boost Voltage Theory, DSPACE, Copper losses, Experimental Work

APPROVAL AND SYMBOLS

<i>symbols</i>	Identifications
<i>DfRM</i>	Doubly fed reluctance machine
<i>DfIM</i>	Doubly fed Induction machine
v_{pds}, v_{pq}	primary direct and quadrature voltage components [V]
v_{sds}, v_{sq}	secondary direct and quadrature voltage components [V]
i_{sds}, i_{sq}	secondary direct and quadrature current components [A]
$\lambda_{pds}, \lambda_{pq}$	primary direct and quadrature flux components [Wb]
$\lambda_{sds}, \lambda_{sq}$	secondary direct and quadrature flux components [Wb]
ω_p, ω_s	primary, secondary winding and rotating frequencies [rad/sec]

I. INTRODUCTION

The induction machine, in applications with limited range of variable speed capability, such as pumps and wind turbines, can be replaced with Brushless Doubly Fed Reluctance Machine (BDFRM) as a potential and substitution solution. [1]. The using of a smaller size inverter in ratio to the machine ratings in BDFRM with low cost afforded, all that has gave it a great attention due their competitive performance [2]. The brushless structure in

BDFRM has brings many benefits in terms of higher reliability and maintenance cost [3]. For what was mentioned previously, the BDFM could be innovative in wind turbine application [4].

In terms of design, the BDFM classified into two kinds: nested cage rotor also called brushless doubly-fed induction machine (BDFIM), and other type that is similar to synchronous reluctance machines [5, 6]. As it mentioned previously, there two windings in stator, one of them is connected to the grid which is known as a primary (power) winding. And the secondary (control) winding is converter fed, with different pole numbers and a salient pole rotor [7] as shown in Figure 1. There is a magnetic coupling between the two stator windings (primary and secondary) with a perfect harmony with the rotation of reluctance rotor, which makes this possible. The essential modulates in the stator MMF waveforms is due to presence of the variable reluctance path of disturbance flux on the machine, corresponding to the flux density harmonics, which can link to the opposite winding [8]. The torque production occurs because of electro-mechanical energy conversion response in the machine [9]. In order to avoid coupling in frequency, BDFRM is designed with different stator pole numbers of primary and secondary windings. Furthermore, the number of rotor poles should be one-half of the total number stator poles [10].

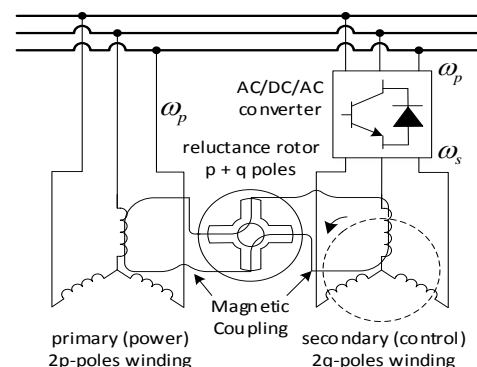


Fig. 1. Configuration of BDFRM

The operational mode flexibility is a very important property of BDFRM (also in DFIM). When shorting the secondary terminals it will operate like an ordinary induction machine. This save behavior will prevent measurements and the inverter from overloading, at starting machine mode. In another case, when the secondary winding supplied with a DC voltage source, the result will be an operation state is similar to ordinary synchronous machine with controlled field coil [11].

The evolution of the concept control complexity, adding to the large number of parameter requirements become one of the reasons which are dictating some power scientists and researchers to adopt the simple control, Capable and stiff especially based on the wind energy conversion system (WECS) Application [12].



Fig. 2. Test rigs units based dSPACE 1103 hardware

This paper will rely on this theory to achieve a dynamic model that contributes to the investigation and confirmation of the validity of this theory. The magnetic-flux in BDFRM should be in a specific level as stated in [13] to induced this flux level, it ought to operate the machine at rated voltage and frequency applied at the same time. However, the speed of machine can control by slip frequency ω_s in secondary side, so that the machine will run in super-speed or sub-synchronous speed depending on the table conditions (1). The plotted speed shows the stability limits of scalar control strategy based BDFRM limitations as a main prospect to develop a control theory with a slight enhancement in term of using boost voltage as motivating voltage to recover the failures in low speed behaviors. The requirement parameters of open loop control assists in sensorless control method, but with low stability.

II. REAL TIME IMPLEMENTATION

The major key to the RTI application programs is the obtaining Simulations software result in the practical field in the laboratory, test its portability with the inverter according to the theory of control algorithm, turn it into a real barometers, and convert it from virtual reality to practice to prove his worth and reality. Implementation software and Control Desk have considered the experiment software. RTI is a Simulink toolbox, which provides blocks to configure models. These blocks allow the users to access to the dSPACE hardware. Control Desk allows, as for it, the users to control and monitor the real-time operation by using many virtual instruments and building a control window when using dSPACE, the several steps required to implement

DS1103 Controller Board is described below Fig. 2. The first step consists in modeling the control system with Simulink and configuring the I/O connections of the Connector Panel thanks to the RTI toolbox. After that, the Real-Time Workshop (RTW) toolbox, using RTI, automatically generates the C-code for the board. Once the execution code has been generated, the dSPACE hardware can perform a real-time experiment, which can be controlled from a PC with Control Desk. Control Desk can be used to monitor the simulation progress, adjust parameters online, capture data (in a format compatible with Matlab) and communicate easily with the upper computer real-time. Dealing with real time application require special software mentioned in [8, 14] to convert the voltage vectors in term Rated voltage and slip angles from the control side with suitable DC link voltage V_{dc} to time vectors T_a and T_b by SVPWM application required [note: the induction mode operation can be obtained by short circuiting the secondary winding or obtained by adjusting vector time position ($T_a T_b T_c$) as $V7 = 111$, or $V0 = 000$), other sectors reflect actual control variables.

III. MATHEMATICAL APPROACH FOR CONTROL ALGORITHMS

Following the dynamic model equations for the BDFRM, permit us to understand the main prospect for scalar control theory.

$$U_p = R_p \dot{i}_p + \frac{d\lambda_p}{dt} \Big|_{\theta_p=cont} + j\omega_p \lambda_s \quad (1)$$

$$U_s = R_s \dot{i}_s + \frac{d\lambda_s}{dt} \Big|_{\theta=cont} + j(\omega_r - \omega_p) \lambda_p \quad (2)$$

The main scope to scalar control application for BDFRM has been considered in mathematical relationship between mechanical rotation angle ω_{rm} and electrical rotation angle ω_r in equation:

$$\omega_{rm} = \frac{\omega_p + \omega_s}{P_r} \leftrightarrow \omega_r = \omega_{rm} P_r = \omega_p + \omega_s \quad (3)$$

The summation of primary and secondary winding frequencies is known as angular velocity ω_r [rad/sec]. Based on these equations can built appropriate rotating frame angle θ_r joined the primary and secondary frame angel in the both side stator winding as follows:

$$\begin{cases} \theta_{rm} = \int \omega_{rm} dt \\ \theta_{p,s} = \int \omega_{p,s} dt \end{cases} \quad (4)$$

$$\theta_r = \theta_{rm} P_r = \theta_p + \theta_s \quad (5)$$

$$\begin{cases} \lambda_p = L_p \dot{i}_p + L_{ps} \dot{i}_s^* e^{j\theta_r} = \lambda_p e^{j\theta_p} \\ \lambda_s = L_s \dot{i}_s + L_{ps} \dot{i}_p^* e^{j\theta_r} = \lambda_s e^{j\theta_s} \end{cases} \quad (6)$$

primary and secondary quantities has been subscripted as 'p&s' respectively. Fig. 3 present complex conjugate for alternative currents inside the BDFRM winding. The frame flew for the secondary voltage start with the stationary angle θ_p in the primary side shifted as rotating angle θ_r to draw secondary voltage angle θ_s .

The vector chart shown in Fig. 3 will describe the orientation of secondary voltage proportion to primary voltage.

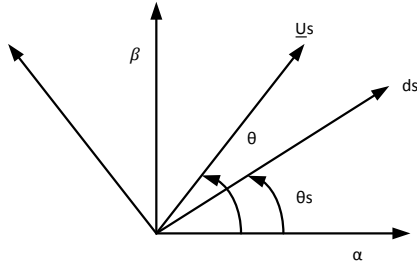


Fig. 3. Phase frame in scalar control

Preceding of the Eq. 3 the secondary slip frequency [rad/second] could appear in a different mod as:

$$\omega_s = \omega_{rm} p_r - \omega_p \quad (7)$$

Slip frequency present as command frequency applied to the secondary side. a positive slip frequency signal will make generated MMF in two-stator windings rotate gradually in the same direction and the machine will increase its speed however negative ω_s means the opposite phase sequence of secondary to primary winding, as shown in Table 1.

TABLE I. SLIP FREQUENCY MODES

Secondary Slip frequency	Mod Operation	Speed Mode
$\omega_s > 0$	Super Synchron-Mode	Super-Sync-Speed >750 to 1000 [rpm]
$\omega_s < 0$	Sub sync-mode	Sub-Sync-Speed < 750 to 500 [rpm]

IV. SCALAR CONTROL OPEN LOOP ALGORITHM

The successes of the scalar control method open loop construction of BDFIM machine consider extra motivation to carry out this study on BDFRM [15]. There are two parts of Scalar Control, one is closed-loop control that normally employs a PI speed controller and the other is open constant voltage/ frequency (V/f) control, this independent control algorithm prepared at a reasonable and appropriate control project quite simple low noise reference speed data thanks to' Sensor less construction, suitable for the system in high-power, heavy-duty and narrow-speed-range applications [16]. The advantage of scalar control is its robustness. However, the high performance will require more accurate control sensors. Both models (open-close) with a little adjustment are considered a real revolution in the field of control management and low cost competitive with efficiency and stiffness related to steady state speed behavior [17].

Desired Speed (reference speed) can adjust speed of the machine throw suitable open loop control algorithm, depended on Eq. 3 as essential method to produce the slip frequency as central command, modified with V/Hertz as a constant ratio of rated voltage to the frequency. Furthermore secondary slip frequencies ω_s intervened as a monitoring value in the control process which identifying the temporary changes in the parameters of control side machine. See Fig. 4.

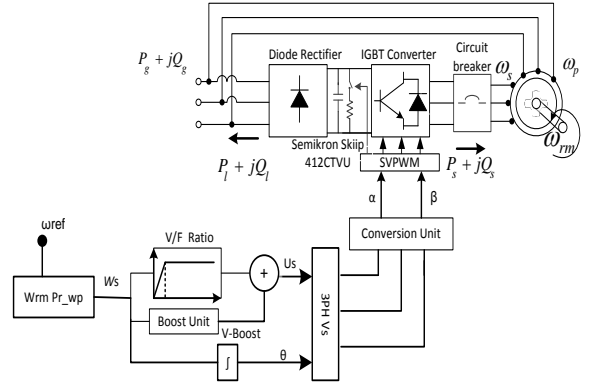


Fig. 4. Open loop control associated with power- electronics

In order to use the principle V/f clarification, the correlation between theoretical approach of dynamic equation and the principle of control should be evaluated our trend to adopt V/f scalar control as a suitable theory concept related to the secondary voltage Eq. 8 in the steady state form:

$$U_s = R_s i_s + j \omega_s \lambda_s = R_s (i_{sd} + j i_{sq}) + j \omega_s \lambda_s \quad (8)$$

For maximizing torque effect, $i_{sd}=0$ the unloaded machine expression will develop to:

$$U_s = j R_s i_{sq} + j \omega_s \lambda_s \quad (9)$$

In case to justify the effect of this variable parameters on the control behavior by neglecting the secondary resistance (large scale Machine) to avoid torque curve distortion in low speed and Maximum power point tracking based WECS application the $\lambda_s \approx \lambda_{ps}$ which can set as equivalent values to $(L_{ps}/L_p \cdot \lambda_p)$ where's λ_p related to the rated primary (volte / frequency).

$$U_s \cong j \omega_s \lambda_{ps} \cong \omega_s \frac{L_{ps}}{L_p} \lambda_p \quad (10)$$

$$\lambda_p \cong \frac{L_{ps}}{L_p} \frac{U_p}{\omega_p} \quad (11)$$

$$U_s \cong \omega_s \frac{L_{ps}}{L_p} \frac{U_p}{\omega_p} \quad (12)$$

Matter of fact the ratio $(L_{ps}/L_p \cdot U_p/\omega_p)$ is the equivalent to constant ratio (V/f) in rest conventional scalar control algorithms. These three Eq. 10, Eq. 11, and Eq. 12 validated the ratio impact on the secondary voltage and distribution of magnetizing flux through machine winding. Furthermore its consider the sole factor for optimizing the efficiency of BFRM machine and copper losses behavior in the next paragraph.

V. MAXIMUM TORQUE PER INVERTER AMPER OPTIMAIZATION

In order to reach positive results in the practice (RTI) application and improve the machine performance to be voluntarily controlled by the open loop control method, the ratio hasn't been taken as an arbitrary value, but calculated according on dynamic equations that govern the machine performance. The value of the secondary current $I_s=I_{sq}$, $I_{sd}=0$) in order to gain maximum magnetizing currents from the primary side. The copper losses on both sides of the machine are expressed in the following form:

$$P_{cup} = \frac{3}{2} R_p i_p^2 \quad (13)$$

$$P_{cus} = \frac{3}{2} R_s i_{sq}^2 \quad (14)$$

The Total copper losses are determined as the sum losses in both sides machine in (super-sub) synchronous mode:

$$P_{cu\ Total} = P_{cup} + P_{cus} \quad (15)$$

The certain values of ratio introduced in rate torque expression could be present the key words to determine the Ratio values with the presence of rated torque (T_r) and rest parameter of BDFRM:

$$T_r = \frac{3}{2} P_r \underbrace{\frac{L_{ps}}{L_p} \lambda_p i_{sq}}_{Ratio} \quad (16)$$

Then it is easy to extract the values of Ratio as below:

$$Ratio = \frac{2}{3 P_r i_{sq}} T_r \quad (17)$$

Substituting the numerical ratio that is obtained from the above equation to the Simulink model Fig. 4, as an approximate Ratio (V/f) value, and tested by reading the amount of the copper losses, on both sides winding of the machine. The optimal value of the Ratio has less copper loss in the machine turns under certain torque and different speed mode. The figures (5, 6, 7 and 8) below tested the system under numeric values about this Ratio the bolt line express the primary losses and the dotted line the secondary losses. Depending on BDFRM theory [18] and inconsistent with the previously mentioned equations open loop Ratio, ($L_p/L_p * U_p/\omega_p$) consider the Maine flux observer. This Ratio should be carefully calculated to maintain a low level of copper losses which cannot be neglected in the term of calculating the efficiency degree of the machine. Therefore this study can be considered to determine the optimal performance of the machine.

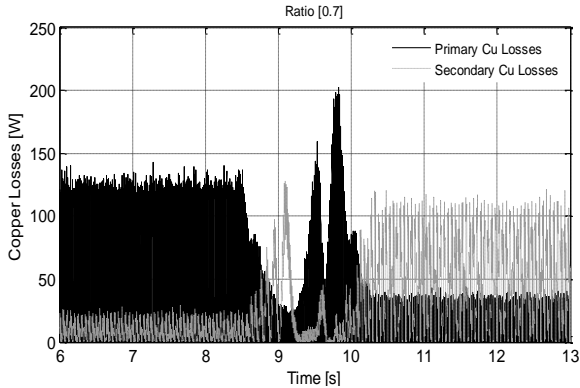


Fig. 5. Copper losses distribution under super-sub sync-speed Ratio 0.7

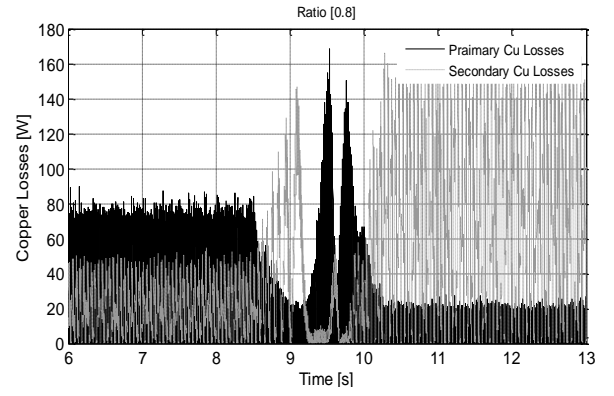


Fig. 6. Copper losses distribution under super-sub sync-speed Ratio 0.8

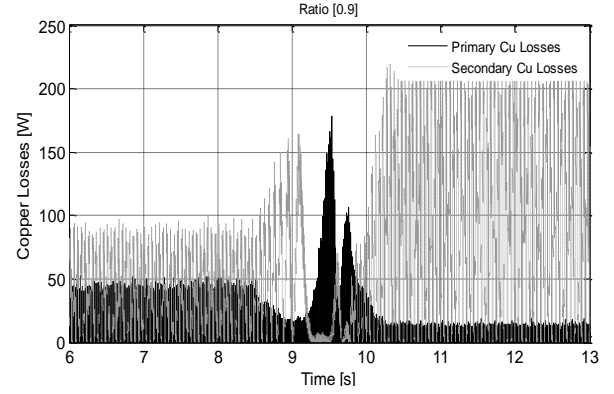


Fig. 7. Cu losses distribution under super-sub sync-speed Ratio 0.9

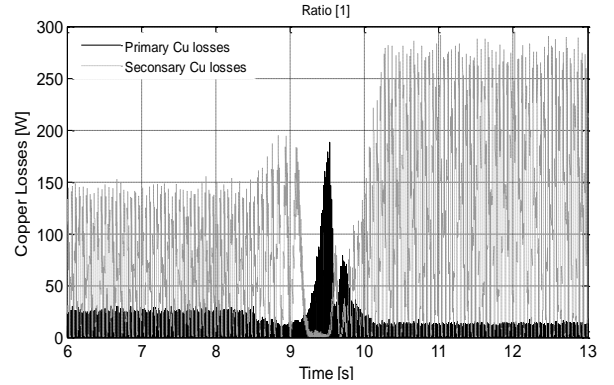


Fig. 8. Cu losses distribution under super-sub sync-speed Ratio 1

The results that had gained from the previous figures (5, 6, 7, 8) in order to find the anticipated Ratio values. The attempts clearly indicate the extent of the impact these Ratios, on the distribution copper losses for both sides of the BDFRM.

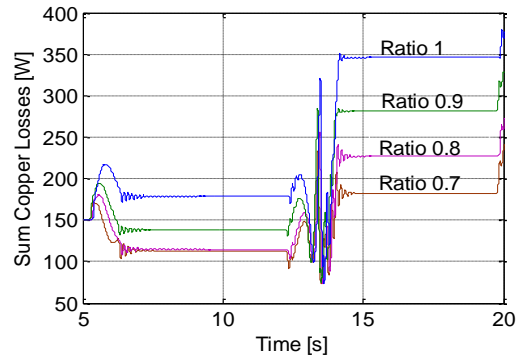


Fig. 9. Simulation results, based multi V/f ratio under same condition

The expected copper losses on both sides converting these variables into a graph form shows the distribution of copper losses on both sides of the machine at each value of the Ratio values and glitches are not affected steady state period.

VI. CONCLUSION

Encouraging of the extracting results the scalar control appearances is easy, strong and flexible for variable desired speed. Other hand the boost voltage has big role to enhance the performance of the machine and support the (sup-sub) synchronous Transaction. The success, which gained from this RTI, is proving the validity of this simple and senseless controller to gate reference speed. other important outcome from this excremental work is confirm the capability of BDFRM to manipulate with multi control algorithms which present this machine as alternative solution for induction machine, synchronous machine and permanent magnate synchronous machine PMSM in manufacture and WECS applications. As concision, scalar control based V/f concenter backup control system for high performance controller (VC & FOC) in faulty case condition, tacking in account decent association with the machine parameters avoiding over speed.

REFERENCES

- [1] H. Luo, Q. Wang, X. Deng, and S. Wan, "A Novel V/f Scalar Controlled Induction Motor Drives with Compensation Based on Decoupled Stator Current," 2006 IEEE International Conference on Industrial Technology, 2006.
- [2] M. G. Mousa, S. M. Allam, and E. M. Rashad, "Sensored and sensorless scalar-control strategy of a wind-driven BDFRG for maximum wind-power extraction," *Journal of Control and Decision*, vol. 5, no. 2, pp. 209–227, 2017.
- [3] A. Rahab, F. Senani, and H. Benalla, "Direct Power Control of Brushless Doubly-fed Induction Generator Used in Wind Energy Conversion System," *International Journal of Power Electronics and Drive Systems (IJPEDS)*, vol. 8, no. 1, p. 417, Jan. 2017.
- [4] L. N. C and A. R., "Design and Experimental Verification of Linear Switched Reluctance Motor with Skewed Poles," *International Journal of Power Electronics and Drive Systems (IJPEDS)*, vol. 6, no. 1, p. 18, Jan. 2015.
- [5] S. Shao, E. Abdi, and R. McMahan, "Low-Cost Variable Speed Drive Based on a Brushless Doubly-Fed Motor and a Fractional Unidirectional Converter," *IEEE Transactions on Industrial Electronics*, vol. 59, no. 1, pp. 317–325, 2012.
- [6] A. Petrushin, M. Tchavychalov, and E. Miroshnichenko, "The Switched Reluctance Electric Machine with Constructive Asymetry," *International Journal of Power Electronics and Drive Systems (IJPEDS)*, vol. 6, no. 1, p. 86, Jan. 2015.
- [7] S. Ademi, M. G. Jovanović, and M. Hasan, "Control of brushless doubly-fed reluctance generators for wind energy conversion systems," *IEEE Trans. Energy Convers.*, vol. 30, DOI 10.1109/TEC.2014.2385472, no. 2, pp. 596-604, Jun. 2015.
- [8] Bakouri, Anass; Mahmoudi, Hassane; Abbou, Ahmed., *Intelligent Control for Doubly Fed Induction Generator Connected to the Electrical Network*, *International Journal of Power Electronics and Drive Systems*; Yogyakarta Vol. 7, Iss. 3, (Sep 2016): 688-700.
- [9] M. Jovanovic, "Optimal performance of brushless doubly fed reluctance machines," 9th International Conference on Electrical Machines and Drives, 1999.
- [10] A. Rahab, H. Benalla1, and F. Senani1 "An overall Control of BDFIG using Direct Power Control for WECS under Unbalanced Grid Voltage Conditions," *International Journal of Engineering Research and Advanced Technology*, vol. 4, no. 3, 2018.
- [11] Y. Liu, W. Xu, K. Yu, and F. Blaabjerg, "A new vector control of brushless doubly-fed induction generator with transient current compensation for stand-alone power generation applications," 2018 IEEE Applied Power Electronics Conference and Exposition (APEC), 2018.
- [12] D. V. Samokhvalov, A. I. Jaber, D. M. Filippov, A. N. Kazak and M. S. Hasan, "Research of Maximum Power Point Tracking Control for Wind Generator," 2020 IEEE Conference of Russian Young Researchers in Electrical and Electronic Engineering (EIConRus), St. Petersburg and Moscow, Russia, 2020, pp. 1301-1305, doi: 10.1109/EIConRus49466.2020.9039180..
- [13] M. Hassan and M. Jovanovic, "Improved scalar control using flexible DC-Link voltage in Brushless Doubly-Fed Reluctance Machines for wind applications," 2012 2nd International Symposium On Environment Friendly Energies And Applications, Newcastle Upon Tyne, UK, 2012, pp. 482-487, doi: 10.1109/EFEA.2012.6294037. International Conference on Power Electronics Systems and Applications, 2011.
- [14] R. Kumar, E. Sulaiman, M. Jenal, and F. S. Bahrim, "Parametric Optimization and Performance Analysis of Outer Rotor Permanent Magnet Flux Switching Machine for Downhole Application," *Journal of Magnetics*, vol. 22, no. 1, pp. 69–77, 2017.
- [15] M. Jovanovic, R. Betz, J. Yu, and E. Levi, "Aspects of vector and scalar control of brushless doubly fed reluctance machines," 4th IEEE International Conference on Power Electronics and Drive Systems. IEEE PEDS 2001- Indonesia. Proceedings (Cat. No.01TH8594), 2002.
- [16] A. Rahab, F. Senani, and H. Benalla, "Direct Power Control of Brushless Doubly-fed Induction Generator Used in Wind Energy Conversion System," *International Journal of Power Electronics and Drive Systems (IJPEDS)*, vol. 8, no. 1, p. 417, Jan 2017.
- [17] M. S. Hasan, A. F. Sharaf, M. D. Albakhait, and A. I. Jaber, "High Performance Rectifier/Multilevel Inverter Based BLDC Motor Drive with PI Controller," *IOP Conference Series: Materials Science and Engineering*, vol. 745, p. 012005, 2020.
- [18] N. E. Ouanjli, A. Derouich, A. E. Ghzizal, Y. E. Mourabit, and M. Taoussi, "Contribution to the Improvement of the Performances of Doubly Fed Induction Machine Functioning in Motor Mode By the DTC Control," *International Journal of Power Electronics and Drive Systems (IJPEDS)*, vol. 8, no. 3, p. 1117, Jan 2017.
- [19] M. Jovanovic, "Brushless doubly fed reluctance machines for low cost variable speed drives," *Proceedings IPEMC 2000. Third International Power Electronics and Motion Control Conference (IEEE Cat. No.00EX435)*, 2000.